Bioresource Technology 451 (2026) 134496

Contents lists available at ScienceDirect

Bioresource Technology

journal homepage: www.elsevier.com/locate/biortech

Residual biodegradable microplastics derived from compostable packaging under large-scale industrial composting fully degrade in soil

Cheick Abou Coulibaly [a,b,c], Sandra Domenek [b,c], Paul Greuet [a,c], Matthieu George [d], Pascale Fabre [d], Rafael Auras [e], Emmanuelle Gastaldi [a,c,*]

[a] UMR IATE, Université de Montpellier, INRAE, L'Institut Agro Montpellier – 2 Place Pierre Viala, 34000 Montpellier, France
[b] Université Paris-Saclay, INRAE, AgroParisTech, UMR SayFood, 91120 Palaiseau, France
[c] Fondation AgroParisTech, Chaire CoPack, 91120 Palaiseau, France
[d] Laboratoire Charles Coulomb, CNRS UMR-5221, Université de Montpellier, Place E. Bataillon, 34095 Montpellier, France
[e] The School of Packaging, Michigan State University, East Lansing, MI 48824, United States

HIGHLIGHTS

- Optimized method for quantifying biodegradable microplastics in compost.
- Analytical workflow validated on full-scale industrial compost samples.
- Near-complete biodegradation confirmed for certified compostable packaging.
- Residual compostable microplastics show complete mineralization in soil.

GRAPHICAL ABSTRACT

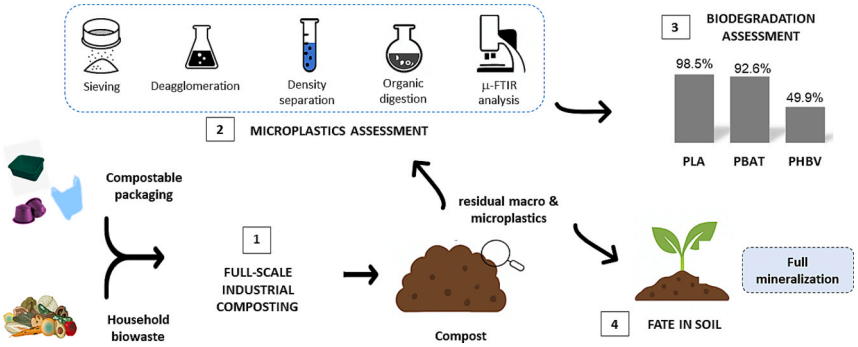

ARTICLE INFO

Keywords:
Compost
Biowaste
Extraction protocol
Infrared microscopy
Material fragmentation

ABSTRACT

The increasing use of compostable plastics in organic waste management calls for reliable analytical tools to verify their complete biodegradation and environmental safety. This study builds upon a previous full-scale composting experiment that monitored the disintegration of certified compostable packaging under industrial composting conditions. A dedicated analytical protocol was optimized and validated to extract, identify, and quantify biodegradable microplastics (BMPs) remaining in the compost. The method combines preconcentration by fractionation, deagglomeration in hot water, density separation with $CaCl_2$, mild oxidative digestion with H_2O_2, and identification by Fourier-transform infrared (FTIR) microscopy. Fragments larger than 35 μm for PBAT and larger than 27 μm for PLA and PHBV were detected. In full-scale industrial composting, the protocol revealed near-complete biodegradation of PLA (98.4 %) and PBAT (92.6 %), whereas PHBV showed partial degradation (49.9 %) due to the structural constraints of the coffee capsule format. Residual BMPs were further assessed under controlled soil conditions, where continued mineralization of PBAT and PHBV confirmed their environmental degradability and low persistence. These findings bridge the gap between disintegration and

* Corresponding author at: UMR IATE, Université de Montpellier, INRAE, L'institut Agro Montpellier – 2 Place Pierre Viala, 34000 Montpellier, France.
E-mail address: emmanuelle.gastaldi@umontpellier.fr (E. Gastaldi).

https://doi.org/10.1016/j.biortech.2026.134496
Received 25 November 2025; Received in revised form 26 January 2026; Accepted 24 March 2026
Available online 24 March 2026

mineralization, providing quantitative evidence of biodegradation from compost to soil and supporting the environmental compatibility of compostable packaging materials.

1. Introduction

Biowaste represents 34 % of municipal solid waste (MSW) in Europe (EEA, 2020), and its sustainable management is a key objective of the European Union's circular economy strategy. Since January 2024, EU directives have mandated source separation of biowaste (EU, 2018) and promoted its treatment through composting and anaerobic digestion (EU, 2024), thereby converting waste into valuable products, such as compost used for soil amendment. Compostable plastics, such as poly (lactic acid) [PLA], poly(butylene adipate-*co*-terephthalate) [PBAT], and poly(3-hydroxybutyrate-*co*-3-hydroxyvalerate) [PHBV], are increasingly used as alternatives to conventional polymers, enabling co-collection of food waste and packaging (EU, 2018). Designed to biodegrade under industrial composting conditions, these materials ultimately mineralise into CO_2, water, and biomass by microorganisms. When correctly managed, they facilitate biowaste collection and reduce contamination of compost streams by non-biodegradable plastics such as polyethylene (PE), polypropylene (PP), and polystyrene (PS) (Edo et al., 2022; Puyuelo et al., 2013).

In our previous study (Gastaldi et al., 2024), we demonstrated that adding 1.28 wt% of certified compostable packaging to biowaste undergoing full-scale industrial composting piles did not disturb the process or compromise the compost quality (Gastaldi et al., 2024). The materials exhibited a mean loss of 98 % after four months, and ecotoxicological assessments confirmed compliance with organic-farming standards (EU, 2019; NF, 2006). However, large-scale assessment focused on macroscopic degradation, leaving the presence and fate of microplastic residues in the final compost unaddressed. Recent studies have shown that even certified compostable plastics may not fully mineralise, and that residual biodegradable microplastics (BMPs) can persist in soil after compost application. For example, Accinelli et al. (2020) found that fragments from compostable carrier bags remained detectable in soil for more than 2 years, while Ruffell et al. (2025) reported measurable levels of BMPs in mature composts. These findings raise concerns about the long-term environmental persistence of BMPs and the need to quantify their transformation beyond the composting stage.

On the other hand, biodegradation involves fragmentation followed by microbial conversion into CO_2, water, and biomass. Laboratory respirometry tests are widely used to quantify CO_2 generation under controlled conditions (ASTM, 2021; Bher et al., 2023; ISO, 2018; Yu and Flury, 2024). However, such setups are impractical in open industrial windrows, where large-scale trials rely on mass-loss measurements. This approach may overestimate biodegradation since regulations only require the quantification of visible plastic fragments > 2 mm (EN, 2000; EU, 2019), while some countries, such as Germany, apply a 1 mm limit (Wiesner et al., 2023). Consequently, smaller microplastics often remain undetected, leading to an incomplete understanding of their actual biodegradation performance.

Micro-Fourier Transform Infrared (μ-FTIR) spectroscopy is the most common technique for microplastic detection and quantification (Dukek et al., 2024; Kotar et al., 2022; Ruffell et al., 2025). Accurate analysis requires efficient extraction and removal of organic matter. Existing protocols, developed for conventional polymers, often use strong oxidative or alkaline treatments unsuitable for biodegradable polymers, which are more sensitive to oxidation and hydrolysis. Compost's high organic content further complicates analysis by clogging filters and interfering with infrared spectra (Ciréderf Boulant et al., 2025; Gouda et al., 2025). Although Fenton's reagent can enhance organic removal (Steiner et al. 2024), it may degrade PLA, PBAT, and PHBV (Ruffell et al., 2025). Hydrogen peroxide (H_2O_2) is a milder alternative, but still leaves 5–13 % of undigested organic matter (Ciréderf Boulant et al. (2025).

Overall, these studies underline the analytical challenge of accurately quantifying BMPs in compost, where organic residues must be removed without damaging the polymers. Optimizing this step is essential to ensure reliable measurement and proper interpretation of compostable plastic biodegradation.

Building upon a previous full-scale industrial composting experiment that focused on the disintegration of certified compostable packaging, the present study introduces a dedicated analytical protocol to extract, identify, and quantify biodegradable microplastics (BMPs) remaining in compost. Accordingly, this work aimed to (i) optimize and validate this protocol (ii) reassess biodegradation under full-scale industrial composting conditions by explicitly accounting for small BMP fractions, and (iii) evaluate the subsequent biodegradation and persistence of residual BMPs in soil.

2. Materials and methods

2.1. Industrial composting operational parameters and compost sampling

Compost samples were collected from two batches from an industrial composting facility (43°38′ N, 3°15′ E) operating with turned open-air windrows. Two batches of compost from the same incoming biowaste were sampled. The first batch ("Materials") contained 1.28 wt% certified compostable packaging to simulate realistic contamination levels, while the second ("Control") received no addition. Both batches were processed under identical composting conditions. As previously reported (Gastaldi et al., 2024), the composting process was carried out in turned open-air windrows, with an active thermophilic phase characterized by average temperatures close to 70 °C (69.7 ∘C ± 2.5 and 69.7 ∘C ± 3.6 in the Control and Materials batches, respectively) lasting approximately 8 weeks, followed by a maturation phase of about 12 weeks. During the active phase, windrows were turned and watered twice a week for the first three weeks and once a week thereafter, while moisture content was maintained around 50 % and pH remained in the alkaline range (≈ 8–9) for both batches. After 4 months, 10 kg of sieved fine compost (< 12 mm) were obtained from each batch by pooling twelve subsamples (~ 1 kg each) collected at different locations within the windrow to ensure spatial representativeness, as described in Gastaldi et al., (2024). Subsequently, all the compost samples were air-dried. A representative 500 g sub-sample was homogenized and fractionated using stacked stainless-steel sieves (Fisherbrand™, France) with mesh sizes of 1.0, 0.8, 0.5, and 0.2 mm to obtain four granulometric fractions. Moisture content was determined gravimetrically (105 °C, 24 h, $n = 3$) using an analytical balance (Mettler Toledo, Switzerland), and fractions were stored in airtight glass jars (see e-supplementary information).

2.2. Extraction protocol for BMPs

Sixteen extraction protocols were evaluated on compost batch "Control", to determine the most effective method for BMP extraction (Table 1). Protocol #1, omitting the deagglomeration step, was included as a negative control to demonstrate its necessity for efficient BMP extraction from aggregated compost matrices. Each protocol combined three steps: (1) Deagglomeration: 1 g of compost with known humidity was mixed with 25 mL water and placed in oven at 50 °C for 1 h; (2) Density separation: deagglomerated compost was mixed with 10 mL of salt solution ($CaCl_2$, $\rho = 1.4$ g/cm^3 or NaI, $\rho = 1.6$ g/cm^3) and centrifuged at 4500 rpm; (3) Oxidative digestion: supernatant was filtered and the residue was digested with 10 mL of either 30 % H_2O_2 (Merck,

Table 1
Tested extraction protocols for BMPs recovery from compost.

	Density separation			Digestion
#	Deagglomeration	Salt solution	Oxidative Reagent	Duration (h)
1	No	$CaCl_2$	Water	1
2	Yes	$CaCl_2$	Water	1
3	Yes	$CaCl_2$	H_2O_2	1
4	Yes	$CaCl_2$	Fenton	1
5	Yes	NaI	Water	1
6	Yes	NaI	H_2O_2	1
7	Yes	NaI	Fenton	1
8	Yes	$CaCl_2$	Water	6
9	Yes	$CaCl_2$	H_2O_2	6
10	Yes	$CaCl_2$	Fenton	6
11	Yes	$CaCl_2$	Water	12
12	Yes	$CaCl_2$	H_2O_2	12
13	Yes	$CaCl_2$	Fenton	12
14	Yes	$CaCl_2$	Water	24
15	Yes	$CaCl_2$	H_2O_2	24
16	Yes	$CaCl_2$	Fenton	24

Note: Water was used as a blank.

Germany) or Fenton's reagent for 1, 6, 12, or 24 h at 50 °C under stirring (see e-supplementary information).

The extraction efficiency was evaluated based on the elimination of inorganic and organic matter, excluding BMPs. Residual material after extraction was used to determine the removal rates at each step. The Separation Rate (*SR*) obtained after the stages of deagglomeration (1) and density separation (2) was calculated using Eq. (1). The Digestion Rate (*DR*) obtained after the oxidative digestion stage (3) was calculated using Eq. (2), according to Mbachu et al. (2021).

$$SR\,(\%) = \frac{m_1 - m_2}{m_1}\,x\,100 \tag{1}$$

$$DR\,(\%) = \frac{m_2 - m_3}{m_2}\,\mathrm{x}\,100 \tag{2}$$

where m_1 is the mass of the initial compost sample expressed as dry matter, m_2 is the mass of the residue after the density separation stage, and m_3 is the mass of the residue after the digestion stage, both recovered by filtration and drying and expressed as dry matter.

The most effective extraction protocol was validated through a spiking test to determine recovery rates. Based on reported microplastic concentrations of 9.5–35 particles per gram dry weight in compost (Edo et al., 2022), 30 fragments (ten reference BMPs per material type) were added to 1 g of compost to simulate realistic contamination levels. The spiked PBAT-based BMPs could be clearly distinguished from the background PBAT residues already present in compost batch "Control". The spiked ones were blue, while the latter—originating from compostable collection bags—were green (see e-supplementary information). The recovery rates expressed in number (*Rn*) or mass (*Rm*) were calculated using Eq. (3) and Eq. (4), according to Prosenc et al., (2021).

$$Rn\,(\%) = \frac{N_{extracted}}{N_{spiked}}\,x\,100 \tag{3}$$

$$Rm\,(\%) = \frac{M_{extracted}}{M_{spiked}}\,x\,100 \tag{4}$$

where N_{spiked} and $N_{\mathrm{extracted}}$ were the number of references BMPs added and recovered after extraction, respectively; M_{spiked} and $M_{\mathrm{extracted}}$ were the mass of reference BMPs added and recovered after extraction, respectively.

Chemical and physical integrity analyses of the recovered BMPs were performed using ATR-FTIR, and microscopic surface characterization (see e-supplementary information).

2.3. BMPs extraction and infrared analysis

The validated protocol was applied to 1 g of compost (wet basis). After deagglomeration, density separation, and digestion, the digestate was vacuum filtered through a 25 μm stainless-steel filter (Xinxiang Xin Ming De Machinery Co., Ltd, China), rinsed with 0.01 wt% Tween 20 solution (Merck, Germany), and transferred onto 0.2 μm Anodisc filters (Whatman®, Cytiva, France). Filter retention performance was verified by analysing the particle size distribution in the filtrate obtained after filtering size-fractionated BMP suspensions (25–50 μm) (e-supplementary information). Filters were dried at 50 °C for 24 h under vacuum and mounted for infrared analysis. Spectral mapping was performed using a μ-FTIR microscope (Nicolet iN10 MX, Thermo Fisher Scientific Inc., USA) equipped with a liquid-nitrogen-cooled MCT detector (Mercury-Cadmium-Telluride). Spectra were acquired in transmission mode using OMNIC Picta® software (Thermo Fisher Scientific, version 1.8.240), generating approximately 45,000 spectra per filter over the 1250–4000 cm^{-1} range, as specified for the Anodisc filter (Löder et al., 2015). BMPs were identified by ≥ 80 % spectral correlation with reference polymers (PLA, PBAT, PHBV) prepared from certified compostable packaging (see e-supplementary information). Particle volume (V, μm^3), was calculated as $V = A \times L$, where A (μm^2) is the projected surface area and L (μm) the particle thickness. Particle mass was derived using polymer densities: PLA (1.25 g/cm^3), PBAT (1.30 g/cm^3), and PHBV (1.28 g/cm^3). Non-biodegradable MPs were identified using siMPle software (Primpke et al., 2019).

2.4. Soil biodegradation of residual BMPs

Residual BMPs (2–5 mm) recovered from the Materials batch were added to agricultural soil (Brittany, France; pH 8.0, organic matter 2.3 %) together with compost from the Control batch at a concentration of 0.6 wt%, simulating an amendment rate of 30 t/ha. The carbon content of BMPs was measured using an elemental analyser (ThermoQuest NA 250, CE Instruments Ltd, UK) to precisely set the plastic dose to 2 mg of carbon from materials per g of soil.

Respirometry tests followed ASTM, 2025, adapted from Chevillard et al., 2011, and were conducted in 1 L hermetically sealed glass vessels (Le Parfait, France) containing a vial with 25 g of soil with 0.6 wt% of compost and 0.4 wt% of BMPs, a vial of 10 mL NaOH (0.1 M; Merck, Germany) to trap CO_2 and a vial of 30 mL distilled water to maintain humidity. CO_2 was quantified by back-titration with HCl (0.1 M; Merck) in the presence of thymolphthalein (0.1 % w/v in ethanol, 95°; Merck), after precipitation with $BaCl_2$ (20 % w/v; Merck).

Biodegradation (*DEG*, %) was calculated as:

$$DEG = \frac{CO_{2\,MPs} - CO_{2\,Blank}}{CO_{2\,max}} \tag{5}$$

$$CO_{2,\,max} = C \times \frac{44.01}{12.01} \tag{6}$$

where C is the amount of carbon in the sample introduced in the amended soil for the test (mg).

All tests were performed in triplicate. Details on setup and modelling are provided in SI-6.

2.5. Statistical analysis

The data were analysed using RStudio (v2024.09). Normality was tested using the Shapiro–Wilk test, and variance homogeneity was tested using Bartlett's test. When normality is satisfied, but the assumption of homogeneity of variances is not, the standard Student's *t*-test and one-way ANOVA were replaced by their variance-robust counterparts: the Welch *t*-test and Welch ANOVA. Accordingly, all comparisons between two groups were performed using the *t*-test, and comparisons involving more than two groups employed ANOVA. The significance threshold

was set at $\alpha = 0.05$ (see e-supplementary information).

2.6. Quality assurance and contamination control

All experiments were conducted under a fume hood while wearing cotton lab coats and powder-free nitrile gloves. Milli-Q water and 0.01 % Tween 20 (Merck) were used for cleaning. Plastic materials were avoided except for centrifuge tubes. Blank tests ($n = 3$) processed Milli-Q water through the full protocol; no BMPs were detected, and only one PE particle (100 μm) was observed in a single replicate. All chemicals were of analytical grade and were purchased from Merck (Germany).

3. Results and discussion

3.1. Optimization of the BMPs extraction protocol

The comparative evaluation of sixteen extraction protocols revealed that compost deagglomeration before density separation significantly improved extraction efficiency (Fig. 1). Without deagglomeration (protocol #1), the separation rate remained below 40 %, whereas protocols including this step (e.g., #2) reached recovery efficiencies above 97 %. Compost aggregates form during air-drying and must be disintegrated to release MPs trapped within the matrix before the density separation stage. Different deagglomeration methods have been described in the literature, such as the use of a dispersing agent under ultrasonic treatment (Goli and Singh, 2023; Wohlleben et al., 2023). However, such treatment can alter the physical and chemical properties of microplastics if energy input or sonication time is not optimized (Goli and Singh, 2023). Instead, the hot water used in this work was sufficient to effectively disperse aggregates (e-supplementary information).

The choice of hypersaline solution also influenced separation performance. Saturated $CaCl_2$ ($\rho = 1.4$ g/cm^3) provided better efficiency than NaI ($\rho = 1.6$ g/cm^3), which tended to float more organic debris and thereby reduce separation efficiency. This is reflected in the higher separation rates (SR) obtained for protocol #2 compared to protocol #5 (97.7 ± 0.2 vs. 48.8 ± 5.3 %). Similar results were observed for protocols #6 and #7 compared to #3 and #4, which also use NaI and yielded lower SR values (42.9 ± 6.7 and 37.7 ± 2.0 %, respectively; see e-supplementary information for statistical analysis). Our findings differ from those of most previous studies. Cutroneo et al., (2021) recommended the use of higher-density saline solution to maximize microplastics recovery across polymers of varying densities, (e.g., PE and PP ~$\rho = 0.9$ g/cm^3; PBAT $\rho = 1.3$ g/cm^3; polyethylene terephthalate (PET) $\rho = 1.4$ g/cm^3; polyvinyl chloride (PVC) $\rho = 1.4$ g/cm^3). In the present case, however, the use of a higher-density solution resulted in greater extraction of undesirable organic matter, as previously reported (Radford et al., 2021; Schütze et al., 2022). Given the high organic matter content of the compost (49.6 to 52.8 wt% dry matter), NaI ($\rho = 1.6$ g/cm^3) caused additional organic material to float, overloading the supernatant and hindering subsequent digestion. The use of even denser solutions such as $ZnCl_2$ ($\rho = 1.7$ g/cm^3) exacerbated this effect further (Ciréderf Boulant et al., 2025; Edo et al., 2022). Moreover, NaI can react exothermically with Fenton's reagent and hydrogen peroxide (Wong and Zhang, 2008). Digestion efficiency depended strongly on the oxidizing agent (Table 1). H_2O_2 achieved higher removal rates, observed for example by comparing protocol #6 and #7 (68 ± 5 % after 1 h to 85 ± 2 % after 24 h) than Fenton's reagent (67 ± 4 % to 75 ± 8 %). Treatment duration had little effect beyond 12 h, as no significant improvement was observed between 12 h and 24 h (compare #12 and #15, see e-supplementary information for statistical analysis).

Despite the overall efficiency of hydrogen peroxide digestion, residual organic matter persisted, likely due to cellulose and lignin, the main structural components of compost, whose contents typically range from 19.6–27.1 % and 39.7–45.1 %, respectively (Gastaldi et al., 2024). These organic materials are well known for their oxidation resistance (Bugg, 2024).

3.2. Validation of polymer integrity and spectral identification

The overall extraction process—particularly oxidative digestion—may alter the physical and chemical properties of BMPs, potentially introducing bias in FTIR analyses. It is therefore essential to evaluate the effects of these treatments on maintaining BMP integrity to ensure accurate μ-FTIR identification and quantification. Surface morphology analysis via SEM revealed that BMPs extracted using the optimized protocol retained their structural integrity (see e-supplementary information). PBAT-based particles exhibited minor surface erosion, likely due to starch digestion, while PLA and PHBV showed

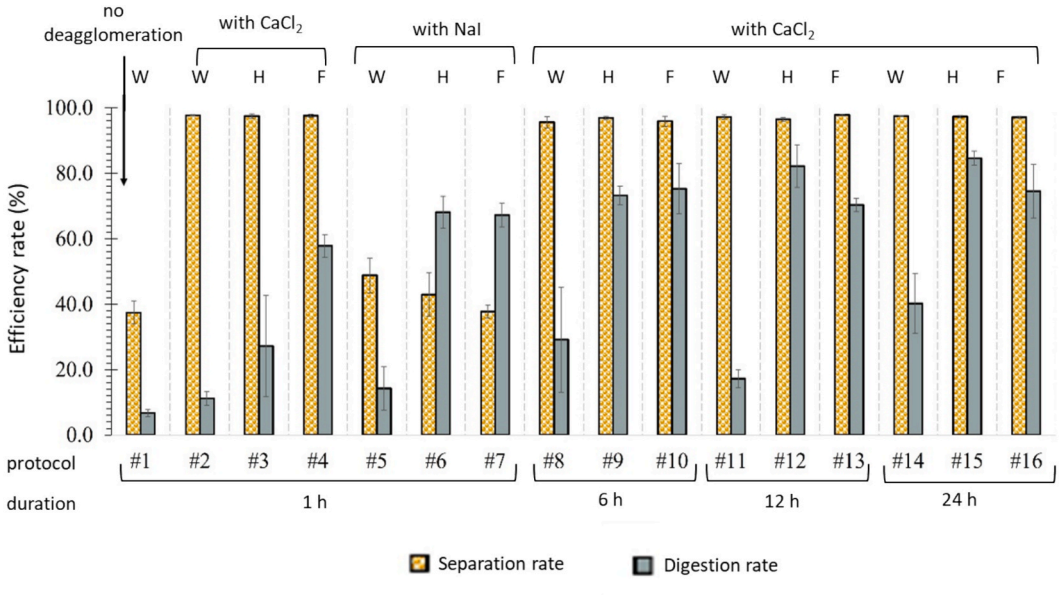

Fig. 1. Density separation and digestion efficiencies for the tested extraction protocols. Error bars represent standard deviations. The letters indicate the digestion reagent used: W for water, H for H_2O_2 and F for Fenton's reagent. Digestion durations are 1 h, 6 h, 12 h, and 24 h. Statistical analysis associated to these data are available in e-supplementary information.

slight surface smoothing without fragmentation. No collapse or cracking was observed, confirming the non-destructive nature of the protocol (see e-supplementary information).

Oxidation of polymer chains during the organic digestion can reduce FTIR identification accuracy, as spectra are compared with reference libraries of the original materials. No oxidation-related changes appeared in the OH stretching region (3100–3700 cm^{-1}) for PLA-, PBAT-based- and PHBV BMPs, regardless of treatment. These results are consistent with changes in carbonyl index (CI) values for PBAT-based and PHBV BMPs, which showed only minor, non-significant variations after 24 h of treatment with H_2O_2 or Fenton reagents. In contrast, for PLA, a small but significant ($p = 0.03$) change in CI was observed after H_2O_2 treatment, indicating early signs of oxidation modification (see e-supplementary information for statistical analysis).

Minor changes were observed for PBAT-based BMPs, with the disappearance of the C=C stretching band (1650–1695 cm^{-1}) and the NH stretching band (3360 cm^{-1}) after treatment. These bands were attributed to Erucamide, a slip agent initially present in the commercial items and lost during composting or extraction. These results differ from those of Al-Azzawi et al., (2020), who reported PLA oxidation showed a narrow band at 3500 cm^{-1}. However, those authors worked at 60 °C (*vs.* 50 °C in this work), which is near the glass transition temperature of PLA and can accelerate reactions.

Correlation analysis showed that all spectra matched their references by more than 80 %, confirming that minor spectral changes did not affect FTIR identification (see e-supplementary information). An 80 % correlation threshold was therefore adopted for subsequent analyses, higher than the 65 % commonly used (Edo et al., 2022; González-Pleiter et al., 2021).

3.3. Evaluation of the recovery rate by spiking tests

The optimized protocol consisted of (1) deagglomeration of compost with water, (2) density separation using $CaCl_2$ ($\rho = 1.4$ g/cm^3), and (3) oxidative digestion with hydrogen peroxide for 12 and 24 h (protocols #12 and #15). Recovery rates of over 98 % by number (Fig. 2a) and 91 % by mass (Fig. 2b) were obtained, regardless of treatment duration or polymer type. This difference between number and mass was attributed to partial digestion and minor particle losses during extraction. Only PBAT shows a statistically significant mass loss (~28 %, $p < 0.001$), consistent with previous reports on oxidative digestion effects (Al-Azzawi et al., 2020; Liu et al., 2023), whereas PLA and PHBV exhibit near-complete recovery (~99–100 %) with no significant losses ($p > 0.05$). Regarding the treatment duration, no significant difference (p-value > 0.05) was observed in the recovery rate at 12–24 h of treatment, either in number or mass. SEM observations showed a smoother surface after oxidative digestion (see e-supplementary information). Nevertheless, the overall extraction process of the most efficient protocol#12, removed most of the organic matter, leaving only 0.6 ± 0.2 % residuals at the end of the procedure. This performance resulted from both the density separation step, which eliminated 96.5 ± 0.6 % of the initial compost, and the digestion step, which further removed 82.2 ± 6.5 % of the remaining material (Fig. 1). The efficiency exceeds that reported by Ciréderf Boulant et al. (2025) who found 5.0–10.7 % undigested residual material. Statistical analyses confirmed that both the saline solution, duration, and digestion reagent significantly influenced extraction efficiency.

To test reproducibility, the optimized extraction protocol was repeated five times, yielding standard deviation (SD) values below 5 %, as shown in Fig. 2. To contextualize protocol robustness, it was compared with other commonly used microplastic extraction techniques in compost and other organic matrices. However, using "clean BMPs" for the spiking test may overestimate extraction efficiency, as real composting conditions alter their properties.

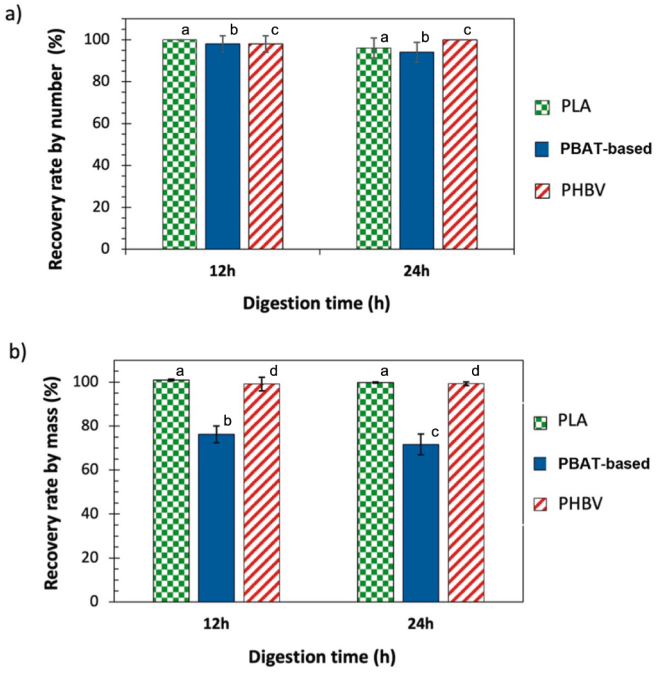

Fig. 2. Recovery rates expressed as number (a) and mass (b) obtained by spiking with the three types of biodegradable reference microplastics: PLA; PBAT-based and PHBV after treatment by digestion with 30 % H_2O_2 for 12 and 24 h. All subscripts are determined by variance analysis with p = 0.05 (Student's *t*-test).

3.4. Microplastics occurrence in industrial compost

The extraction method was applied to assess the concentration of MPs, including BMPs, in the "Materials" and "Control" batches collected from a full-scale industrial composting facility. Analysis of both composts revealed the presence of conventional and biodegradable MPs.

The mass concentration of conventional non-biodegradable MPs recovered from the "Control" batch corresponded to 9.1 ± 6.9 items g^{-1} (see e-supplementary information). Conversely, only small quantities of conventional MPs were detected in the "Materials" batch, with concentrations of 1.9 ± 1.9 μg g^{-1}, corresponding to 0.3 ± 0.3 items g^{-1}. This low contamination level reflects the systematic removal of conventional packaging materials during composting. In terms of particle number, PE was the most abundant conventional polymer, with 8.4 ± 6.9 particles g^{-1} in the "Control" batch and 0.4 ± 0.4 particles g^{-1} in the "Materials" batch, mainly in the 0.2–0.5 mm size fraction. The concentrations obtained in the "Control" batch for conventional MPs were of the same order of magnitude as those reported by Edo et al. 2022, who found 10–30 plastic particles g^{-1} dry mass (< 2 mm), depending on the composting plant and sampling period.

PBAT BMPs were detected in the "Control" batch (Table 2). Since no compostable material was intentionally added there, they likely originated from the degradation of compostable bags used for household biowaste collection. No PLA or PHBV BMPs were detected in the "Control" batch, as expected, since packaging made from these two polymers is still rarely used in France. The biowaste from the "Materials" batch initially contained 1.28 wt% compostable plastics, corresponding to 2.3 wt% on a dry-matter basis. The calculated initial polymer concentrations were: 6750 μg. g^{-1} PLA, 14700 μg. g^{-1} PBAT and 1590 μg. g^{-1} PHBV. Table 2 shows that BMPs from these three polymers were recovered after composting. All PLA BMPs were found in the two largest size fractions, whereas most PBAT BMPs (> 76 %) were recovered in the smallest size fractions, reflecting the extensive disintegration of PBAT-based materials. PHBV BMPs corresponded mainly to particles larger than 0.5 mm (67 %). Although the detection of residual BMPs in compost has raised concerns regarding micro- and nanoplastic

Table 2
Concentrations in number and mass of biodegradable microplastics in the 'Materials' and 'Control' compost batches.

		BMPs concentration in number (items. g^{-1} dry mass) Mean ± SD ($n = 3$)			BMPs concentration in mass (µg. g^{-1} dry mass) Mean ± SD ($n = 3$)		
Compost batch	Size fraction (mm)	PLA	PBAT-based	PHBV	PLA	PBAT-based	PHBV
"Control"	[1.0–0.8]	nd	6.1 ± 0.7	nd	nd	23.8 ± 11.2	nd
	[0.8–0.5]	nd	12.1 ± 2.2	nd	nd	45.6 ± 25.9	nd
	[0.5–0.2]	nd	17.3 ± 6.3	nd	nd	50.3 ± 36.9	nd
	[0.2–0.03]	nd	11.3 ± 3.5	nd	nd	31.4 ± 4.0	nd
	Total	nd	46.8 ± 7.6	nd	nd	151.1 ± 46.6	nd
"Materials"	[1.0–0.8]	0.2 ± 0.1	8.4 ± 1.3	0.1 ± 0.1	9.3 ± 8.8	111.0 ± 37.9	32.4 ± 30.2
	[0.8–0.5]	0.04 ± 0.07	12.7 ± 0.3	0.2 ± 0.1	2.3 ± 3.9	107.4 ± 2.4	56.8 ± 31.9
	[0.5–0.2]	nd	56.7 ± 3.9	0.5 ± 0.0	nd	361.4 ± 66.4	42.9 ± 6.2
	[0.2–0.03]	nd	27.4 ± 1.5	nd	nd	201.4 ± 45.7	nd
	Total	0.2 ± 0.1	105.2 ± 4.4	0.8 ± 0.1	11.6 ± 10.9	781.2 ± 89.1	132.1 ± 44.4

SD is the standard deviation and n = 3 is the sample size.
nd: not detected.
PLA: polylactic acid; PBAT: poly(butylene adipate-co-terephthalate); PHBV: poly(hydroxybutyrate-*co*-valerate).

formation (Accinelli et al., 2020; Ruffell et al., 2025), it is essential to distinguish transient degradation intermediates from true environmental persistence. Unlike conventional plastics (Edo et al., 2022), biodegradable polymers undergo continuous microbial assimilation, and the formation of micro- and nano-sized fragments represents a natural intermediate step leading to complete mineralization (Mohanan et al., 2020).

3.5. Biodegradation performance based on BMP mass balance

Biodegradation was calculated from the mass loss of the different polymers using the data of Table 2 and the recovery rates obtained in our previous study. The results are summarized in Table 3.

Recovered PLA BMPs represented 0.1 ± 0.1 wt% of the initial PLA mass added to the biowaste (Table 3). Including the recovery rate for fragments > 1 mm, it can be concluded that 98.5 ± 0.2 % of the initial PLA was biodegraded. PBAT-based BMPs originated both from intentionally added materials and from PBAT-based compostable collection bags. Since the two sources could not be distinguished, the recovery rate was calculated only from intentionally added PBAT, subtracting the values obtained in the "Control" batch. The resulting BMP recovery rate was 4.3 ± 0.6 wt%, indicating that 92.6 ± 0.6 wt% of the PBAT-based materials were biodegraded. For PHBV, only 49.8 ± 2.8 wt% of the materials initially added, was biodegraded.

Table 3
Mass ratio between residual fragments recovered in compost and the mass of packaging materials initially added to biowaste before composting under large-scale conditions.

Residual fragments after composting	Size fraction (mm)	Materials Mean (%) ± SD ($n = 3$)		
		PLA	PBAT	PHBV
Recovery as BMPs	[1.0–0.8]	0.1 ± 0.1	0.6 ± 0.3	2.1 ± 1.9
	[0.8–0.5]	0.03 ± 0.06	0.4 ± 0.2	3.6 ± 2.0
	[0.5–0.2]	nd	2.1 ± 0.3	2.7 ± 0.4
	[0.2–0.03]	nd	1.2 ± 0.3	nd
Total BMPs	**[1.0–0.03]**	**0.1 ± 0.1**	**4.3 ± 0.6**	**8.4 ± 2.8**
Recovery as large fragments[a]	[12.0–1.0]	1.4	3.1	41.8
Total all residual fragments	[12.0–0.03]	1.5 ± 0.2	7.4 ± 0.6	50.2 ± 2.8
Total Biodegradation (%)		**98.5 ± 0.2**	**92.6 ± 0.6**	**49.8 ± 2.8**

SD is the standard deviation and $n = 3$ is the sample size.
nd: not detected.
[a] Total large fragments recovered during a previous study.

The biodegradation rates of PLA and PBAT-based materials exceeded the threshold for ultimate biodegradation specified in NF EN 13432 (EN, 2000), confirming their excellent performance under full-scale industrial composting conditions. In the present study, the high biodegradation rates reflect the sustained thermophilic conditions achieved during full-scale composting (≈45 days at ~ 70 °C), which were shorter than the maximum 6 months specified in NF EN 13432 (EN, 2000) but conducted at a higher temperature (70 °C versus 58 °C). Such conditions strongly promoted biodegradation, as elevated temperatures enhance hydrolytic cleavage of ester bonds and microbial assimilation of PLA, with degradation rates increasing exponentially above 55 °C (Karamanlioglu et al., 2017). Under these conditions, similar temperature profiles in Control and Materials batches indicate that compostable packaging did not hinder composting performance. It is worth noting that this composting experiment represents a worst-case scenario, as all materials were unused and had not been in contact with spoiled food waste. In addition, PBAT formulations are known to vary in composition (Suarez Murcia et al., 2025), particularly in starch content, which can enhance disintegration and biodegradation due to rapid starch degradation. FTIR analysis of BMPs confirmed the absence of starch in PBAT-based fragments.

Unlike PLA and PBAT-based materials, PHBV did not meet the biodegradation threshold of NF EN 13432 (EN, 2000). This PHBV material originated from new and empty coffee capsules, which were thicker (720–1200 µm) and geometrically less favourable for microbial colonization than PBAT-based bags. The limited biodegradation observed under full-scale industrial composting conditions is therefore likely due to geometric constraints rather than an intrinsic limitation of the polymer itself.

3.6. Environmental fate of residual BMPs in soil

Incomplete biodegradation of compostable materials under industrial composting conditions raises questions about the environmental fate of residual BMPs once compost is applied to soil. To address this, the biodegradation of PBAT and PHBV particles recovered from compost was evaluated under controlled laboratory conditions, following the standardized soil respirometry protocol (EN, 2018). Due to the high biodegradability of PLA and the limited quantity of recovered PLA BMPs, soil biodegradation tests could not be performed for this polymer. The mineralization kinetics are shown in Fig. 3, and the model parameters obtained from Hill's sigmoid equation are summarized in Table 4.

Validation of the Respirometry test using cellulose confirmed its reliability, achieving 70 % mineralization within 70 days—well below the 183-day threshold required by the standard. Both PBAT- and PHBV-

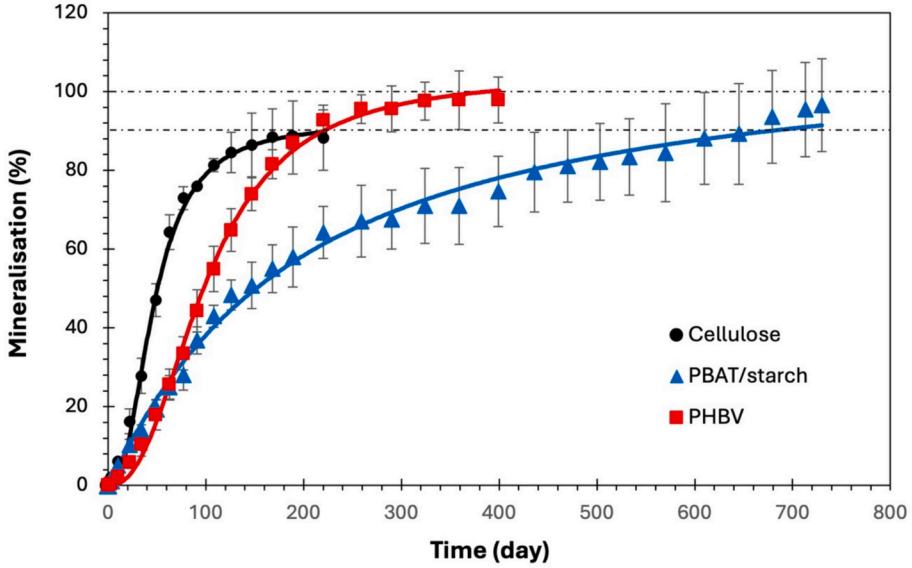

Fig. 3. Respirometry biodegradation kinetics of PBAT- and PHBV-based microplastics [0.5–0.2 mm] from the "Materials" batch under soil conditions at 28 °C. Symbols are experimental data points. Solid and dot lines correspond to the modelling of the curve using Hill's sigmoid function for PBAT-based BMP, PHBV-based BMP, and cellulose. Error bars represent the confidence intervals with a = 0.05. The mineralization threshold values (≥ 90 %) required by EN 17033 (2018) are indicated by dotted lines.

Table 4
Hill parameters of the modelling of biodegradation curves of BMPs in soil.

Sample	Deg_{max} (%) Mean ± SD	*k* (day)	*n*	R^2
Control (cellulose)	92.0 ± 1.5	46.0 ± 1.2	2.4 ± 0.1	0.99
PHBV	104.1 ± 1.5	100.9 ± 2.0	2.4 ± 0.1	0.99
PBAT-based	112.7 ± 5.3	186.7 ± 19.7	1.1 ± 0.1	0.99

R2 is the coefficient of determination for the fit using Hill's equation.
SD is the standard deviation and $n = 3$ is the sample size.

based BMPs exhibited continuous mineralization over two years, demonstrating their biodegradability in soil achieving more than 90 % mineralization, and meeting the EN 17033 (EN, 2018) criterion for full biodegradability. As prescribed by standardized respirometric methods, mineralization was assessed by CO_2 evolution; non-mineralized polymer carbon is therefore most likely transiently accumulated in microbial biomass. However, the degradation rates differed markedly between the two polymers. PHBV microplastics mineralized faster, with a half-degradation time (*k*) of about 101 days, compared to 187 days for PBAT. The faster mineralization of PHBV in soil (Fig. 3) contrasts with its limited biodegradation during composting (Table 3), confirming that the poor performance under composting mainly results from insufficient disintegration of the commercial items rather than from the polymer's intrinsic properties. The use of larger BMP fragments (2–5 mm) represents a conservative worst-case scenario, as larger particles exhibit lower specific surface area and slower microbial colonization (Mohanan et al., 2020). Consequently, the observed mineralization rates are expected to underestimate the degradation of smaller residual BMPs (< 0.5 mm) recovered after composting. In addition, recovering sufficient amounts of these small residual BMPs from compost to conduct soil mineralization experiments in compliance with standard requirements is highly challenging. Larger, well-defined BMP fragments were therefore selected to ensure methodological robustness and reproducibility. Overall, these results indicate that residual BMPs from compost continue to biodegrade after land application, confirming their limited persistence in soil. However, small particles and oligomers below the detection limit may remain.

4. Conclusion

This study presents a validated, reproducible analytical protocol for quantifying biodegradable microplastics (BMPs) in compost. The optimized method combines hot water deagglomeration, $CaCl_2$ density separation ($\rho = 1.4$ g/cm^3), and mild H_2O_2 digestion (30 %, 50 °C, 12 h), followed by μ-FTIR identification. It demonstrates high efficiency in organic-rich matrices, enabling the detection of particles larger than 35 μm for PBAT and larger than 27 μm for PLA and PHBV, without compromising polymer integrity.

In full-scale industrial composting, the protocol revealed near-complete biodegradation of PLA (98.5 %) and PBAT (92.6 %), whereas PHBV showed partial degradation (49.8 %) due to the structural constraints of the coffee capsule format. Residual BMPs were further assessed under controlled soil conditions, where continued mineralization of PBAT and PHBV confirmed their environmental degradability and low persistence. These findings bridge the gap between disintegration and mineralization, providing quantitative evidence of the continuity of biodegradation from compost to soil.

Although high mineralization rates and the predominance of fine BMP residues are indicative of limited long-term accumulation in soil under repeated compost application, future research should expand polymer coverage, explore advanced composting technologies, investigate nano- and microparticles ≤ 27 μm, conduct multi-cycle field studies, further assess PLA residues, and evaluate the influence of PHBV material geometries to strengthen end-of-life assessment.

Overall, this work strengthens the scientific basis for sustainable packaging design and contributes to harmonizing end-of-life assessment protocols within circular bioresource systems, with direct applicability to future compostability certification frameworks through the inclusion of microplastic quantification.

Declaration of generative AI and AI-assisted technologies in the writing process

During the preparation of this work, the corresponding author used DeepL and ChatGPT to assist in translation and language refinement. After using these tools, the author reviewed and edited the content as needed and takes full responsibility for the final version of the

manuscript.

CRediT authorship contribution statement

Cheick Abou Coulibaly: Writing – review & editing, Writing – original draft, Methodology, Investigation, Formal analysis, Data curation, Conceptualization. **Sandra Domenek:** Writing – review & editing, Writing – original draft, Validation, Project administration, Methodology, Investigation, Funding acquisition, Conceptualization. **Paul Greuet:** Methodology, Investigation, Data curation. **Matthieu George:** Writing – review & editing, Validation, Project administration, Investigation, Funding acquisition, Conceptualization. **Pascale Fabre:** Writing – review & editing, Validation, Project administration, Investigation, Funding acquisition, Conceptualization. **Rafael Auras:** Writing – review & editing, Validation, Supervision. **Emmanuelle Gastaldi:** Writing – review & editing, Writing – original draft, Validation, Supervision, Project administration, Methodology, Investigation, Funding acquisition, Conceptualization.

Declaration of competing interest

The authors declare that they have no known competing financial interests or personal relationships that could have appeared to influence the work reported in this paper.

Acknowledgments

This study was conducted as part of the CIPROP project, with financial support from the French Agency for Food, Environmental and Occupational Health & Safety (ANSES, France) under the PNR-EST programme; the BIOFRAG project, with financial support from LabEx NumEv, University of Montpellier; and the Mineral project, with financial support from the Foundation of AgroParisTech, which hosts the philanthropic partnership Chair CoPack. The authors would like to thank the team at Syndicat Centre Hérault (Aspiran, France) for hosting the large-scale experiment at its composting plant and for its support in implementing the overall composting process. The authors also thank Prof. Stéphane Peyron (IATE, University of Montpellier) for providing access to the infrared microscopy equipment used in this study and for valuable discussions on the methodological approach.

Appendix A. Supplementary data

Supplementary data to this article can be found online at https://doi.org/10.1016/j.biortech.2026.134496.

Data availability

Data will be made available on request.

References

Accinelli, C., Abbas, H.K., Bruno, V., Nissen, L., Vicari, A., Bellaloui, N., Little, N.S., Thomas Shier, W., 2020. Persistence in soil of microplastic films from ultra-thin compostable plastic bags and implications on soil *Aspergillus flavus* population. Waste Manag. 113, 312–318. https://doi.org/10.1016/j.wasman.2020.06.011.

Al-Azzawi, M.S.M., Kefer, S., Weißer, J., Reichel, J., Schwaller, C., Glas, K., Knoop, O., Drewes, J.E., 2020. Validation of sample preparation methods for microplastic analysis in wastewater matrices—reproducibility and standardization. Water 12, 2445. https://doi.org/10.3390/w12092445.

ASTM, 2025. D5988-18. Standard Test Method for Determining Aerobic Biodegradation of Plastic Materials in Soil. doi:10.1520/D5988-18R25.

ASTM, 2021. D5338-15. Standard Test Method for Determining Aerobic Biodegradation of Plastic Materials Under Controlled Composting Conditions, Incorporating Thermophilic Temperatures. doi:10.1520/D5338-15R21.

Bher, A., Cho, Y., Auras, R., 2023. Boosting degradation of biodegradable polymers. Macromol. Rapid Commun. 44, 2200769. https://doi.org/10.1002/marc.202200769.

Bugg, T.D.H., 2024. The chemical logic of enzymatic lignin degradation. Chem. Commun. 60, 804–814. https://doi.org/10.1039/D3CC05298B.

Chevillard, A., Angellier-Coussy, H., Cuq, B., Guillard, V., César, G., Gontard, N., Gastaldi, E., 2011. How the biodegradability of wheat gluten-based agromaterial can be modulated by adding nanoclays. Polym. Degrad. Stab. 96, 2088–2097. https://doi.org/10.1016/j.polymdegradstab.2011.09.024.

Ciréderf Boulant, D., Simon, M., Magueresse, A., Mortas, N., Thévenin, N., Yeuch, V., Durand, G., Caurant, A., Goulitquer, S., Even, A., Maisonnat, S., Yesbergenova-Cuny, Z., Deportes, I., Bruzaud, S., Kedzierski, M., 2025. Method validation: extraction of microplastics from organic fertilisers. Environments 12, 143. https://doi.org/10.3390/environments12050143.

Cutroneo, L., Reboa, A., Geneselli, I., Capello, M., 2021. Considerations on salts used for density separation in the extraction of microplastics from sediments. Mar. Pollut. Bull. 166, 112216. https://doi.org/10.1016/j.marpolbul.2021.112216.

Dukek, P., Schleheck, D., Kovermann, M., 2024. High-resolution NMR spectroscopic approaches to quantify PET microplastics pollution in environmental freshwater samples. Chemosphere 367, 143657. https://doi.org/10.1016/j.chemosphere.2024.143657.

Edo, C., Fernández-Piñas, F., Rosal, R., 2022. Microplastics identification and quantification in the composted organic fraction of municipal solid waste. Sci. Total Environ. 813, 151902. https://doi.org/10.1016/j.scitotenv.2021.151902.

EEA, 2020. European Environment Agency, Bio-waste in Europe: turning challenges into opportunities. Publications Office, LU.

EN, 2018. EN 17033 : 2018 Plastics - Biodegradable mulch films for use in agriculture and horticulture - Requirements and test methods.

EN, 2000. EN 13432 : 2000 Requirements for packaging recoverable through composting and biodegradation.

EU, 2024. Regulation EU 2025/40 of the European Parliament and of the Council of 19 December 2024 on packaging and packaging waste, amending Regulation (EU) 2019/1020 and Directive (EU) 2019/904, and repealing Directive 94/62/EC (Text with EEA relevance).

EU, 2019. Regulation EU 2019/1009 of the European Parliament and of the Council of 5 June 2019 laying down rules on the making available on the market of EU fertilising products and amending Regulations (EC) No 1069/2009 and (EC) No 1107/2009 and repealing Regulation (EC) No 2003/2003.

EU, 2018. Directive EU 2018/851 of the European Parliament and of the Council of 30 May 2018 amending Directive 2008/98/EC on waste.

Gastaldi, E., Buendia, F., Greuet, P., Benbrahim Bouchou, Z., Benihya, A., Cesar, G., Domenek, S., 2024. Degradation and environmental assessment of compostable packaging mixed with biowaste in full-scale industrial composting conditions. Bioresour. Technol. 400, 130670. https://doi.org/10.1016/j.biortech.2024.130670.

Goli, V.S.N.S., Singh, D.N., 2023. Effect of ultrasonication conditions on polyethylene microplastics sourced from landfills: a precursor study to establish guidelines for their extraction from environmental matrices. J. Hazard. Mater. 459, 132230. https://doi.org/10.1016/j.jhazmat.2023.132230.

González-Pleiter, M., Edo, C., Aguilera, Á., Viúdez-Moreiras, D., Pulido-Reyes, G., González-Toril, E., Osuna, S., De Diego-Castilla, G., Leganés, F., Fernández-Piñas, F., Rosal, R., 2021. Occurrence and transport of microplastics sampled within and above the planetary boundary layer. Sci. Total Environ. 761, 143213. https://doi.org/10.1016/j.scitotenv.2020.143213.

Gouda, M.Z., Roberge, S., Khiari, L., Benjannet, R., Desrosiers, M., 2025. Novel integrated workflow for microplastics extraction, quantification, and characterization in organic fertilizing residuals using micro-Fourier transform infrared spectroscopy (μ-FTIR). Chemosphere 377, 144357. https://doi.org/10.1016/j.chemosphere.2025.144357.

ISO, 2018. ISO 14855-2: 2018 Determination of the ultimate aerobic biodegradability of plastic materials under controlled composting conditions — Method by analysis of evolved carbon dioxide Part 2: Gravimetric measurement of carbon dioxide evolved in a laboratory-scale test.

Karamanlioglu, M., Preziosi, R., Robson, G.D., 2017. Abiotic and biotic environmental degradation of the bioplastic polymer poly(lactic acid): a review. Polym. Degrad. Stab. 137, 122–130. https://doi.org/10.1016/j.polymdegradstab.2017.01.009.

Kotar, S., McNeish, R., Murphy-Hagan, C., Renick, V., Lee, C.-F.-T., Steele, C., Lusher, A., Moore, C., Minor, E., Schroeder, J., Helm, P., Rickabaugh, K., De Frond, H., Gesulga, K., Lao, W., Munno, K., Thornton Hampton, L.M., Weisberg, S.B., Wong, C. S., Amarpuri, G., Andrews, R.C., Barnett, S.M., Christiansen, S., Cowger, W., Crampond, K., Du, F., Gray, A.B., Hankett, J., Ho, K., Jaeger, J., Lilley, C., Mai, L., Mina, O., Lee, E., Primpke, S., Singh, S., Skovly, J., Slifko, T., Sukumaran, S., van Bavel, B., Van Brocklin, J., Vollnhals, F., Wu, C., Rochman, C.M., 2022. Quantitative assessment of visual microscopy as a tool for microplastic research: recommendations for improving methods and reporting. Chemosphere 308, 136449. https://doi.org/10.1016/j.chemosphere.2022.136449.

Liu, H., Jiao, Q., Pan, T., Liu, W., Li, S., Zhu, X., Zhang, T., 2023. Aging behavior of biodegradable polylactic acid microplastics accelerated by UV/H2O2 processes. Chemosphere 337, 139360. https://doi.org/10.1016/j.chemosphere.2023.139360.

Löder, M.G.J., Kuczera, M., Mintenig, S., Lorenz, C., Gerdts, G., 2015. Focal plane array detector-based micro-Fourier-transform infrared imaging for the analysis of microplastics in environmental samples. Environ. Chem. 12, 563. https://doi.org/10.1071/EN14205.

Mbachu, O., Jenkins, G., Pratt, C., Kaparaju, P., 2021. Enzymatic purification of microplastics in soil. MethodsX 8. https://doi.org/10.1016/j.mex.2021.101254.

Mohanan, N., Montazer, Z., Sharma, P.K., Levin, D.B., 2020. Microbial and enzymatic degradation of synthetic plastics. Front. Microbiol. 11, 580709. https://doi.org/10.3389/fmicb.2020.580709.

NF, 2006. NF U44-051:2006-Organic soil improvers-Designations, specifications and marking.

Primpke, S., Dias, A., Gerdts, G., 2019. Automated identification and quantification of microfibres and microplastics. Anal. Methods 11, 2138–2147. https://doi.org/10.1039/C9AY00126C.

Prosenc, F., Leban, P., Šunta, U., Kralj, M.B., 2021. Extraction and identification of a wide range of microplastic polymers in soil and compost. Polymers 13. https://doi.org/10.3390/polym13234069.

Puyuelo, B., Colón, J., Martín, P., Sánchez, A., 2013. Comparison of compostable bags and aerated bins with conventional storage systems to collect the organic fraction of municipal solid waste from homes. A Catalonia case study. Waste Manag. 33, 1381–1389. https://doi.org/10.1016/j.wasman.2013.02.015.

Radford, F., Zapata-Restrepo, L.M., Horton, A.A., Hudson, M.D., Shaw, P.J., Williams, I. D., 2021. Developing a systematic method for extraction of microplastics in soils. Anal. Methods 13, 1695–1705. https://doi.org/10.1039/D0AY02086A.

Ruffell, H., Pantos, O., Robinson, B., Gaw, S., 2025. Quantification of microplastics in biowastes including biosolids, compost, and vermicompost destined for land application. Water Emerg Contam Nanoplastics 4. https://doi.org/10.20517/wecn.2024.65.

Schütze, B., Thomas, D., Kraft, M., Brunotte, J., Kreuzig, R., 2022. Comparison of different salt solutions for density separation of conventional and biodegradable microplastic from solid sample matrices. Environ. Sci. Pollut. Res. 29, 81452–81467. https://doi.org/10.1007/s11356-022-21474-6.

Steiner, T., Leitner, L.-C., Zhang, Y., Möller, J.N., Löder, M.G.J., Greiner, A., Laforsch, C., Freitag, R., 2024. Detection and specific chemical identification of submillimeter plastic fragments in complex matrices such as compost. Sci. Rep. 14, 2282. https://doi.org/10.1038/s41598-024-51185-6.

Suarez Murcia, J.C., Huet, G., Lamarque, J., Gastaldi, E., Sambusiti, C., Puchelle, V., Grassl, B., Domenek, S., Monlau, F., 2025. Chemical composition and mesophilic anaerobic digestion of commercial compostable food packaging: Implications for bio-waste management. Bioresour. Technol. 424, 132273. https://doi.org/10.1016/j.biortech.2025.132273.

Wiesner, Y., Bednarz, M., Braun, U., Bannick, C.G., Ricking, M., Altmann, K., 2023. A promising approach to monitor microplastic masses in composts. Front. Environ. Chem. 4, 1281558. https://doi.org/10.3389/fenvc.2023.1281558.

Wohlleben, W., Rückel, M., Meyer, L., Pfohl, P., Battagliarin, G., Hüffer, T., Zumstein, M., Hofmann, T., 2023. Fragmentation and mineralization of a compostable aromatic–aliphatic polyester during industrial composting. Environ. Sci. Technol. Lett. 10, 698–704. https://doi.org/10.1021/acs.estlett.3c00394.

Wong, G.T.F., Zhang, L.-S., 2008. The kinetics of the reactions between iodide and hydrogen peroxide in seawater. Mar. Chem. 111, 22–29. https://doi.org/10.1016/j.marchem.2007.04.007.

Yu, Y., Flury, M., 2024. Unlocking the potentials of biodegradable plastics with proper management and evaluation at environmentally relevant concentrations. Npj Mater. Sustain. 2, 9. https://doi.org/10.1038/s44296-024-00012-0.